

Analysis of Dissipative Incompressible Heat-Generating Fluid with Coupled Mass and Heat Transfer over a Semi-Infinite Horizontal Plate

Kaari Catherine¹ and Kirimi Jacob²

¹University Of Embu, P.O Box 6-60100, Embu, Kenya
h.kirimi@yahoo.com

²Chuka University, P.O. Box 109-60400, Chuka, Kenya
kettyc98@yahoo.com

Abstract

We investigate the magneto hydrodynamics stokes' problem for a viscous dissipative incompressible heat generating fluid with mass and heat transfer. The momentum, energy, and concentration equations are non - dimensionalized resulting in the governing parameters; Grashof number (Gr), Prandtl number (Pr), Eckert number (Ec) and Schmidt number (Sc). The temperature and concentration distribution together with their behaviour for different variations in the governing parameters are obtained. The partial differential equations governing the problem are discretized using finite difference method and the results obtained analyzed using tables and graphs.

Keywords: Heat transfer, Mass transfer, MHD flow, Boundary layer

1. Introduction

A comprehensive study on the analysis of heat transfer in viscous heat generating fluid is important in engineering processes pertaining to flow in which a fluid supports an exothermic chemical or nuclear reaction or in problems concerned with dissociating fluids.

The volumetric heat generation has been assumed to be constant or function of space variable. Another class of problems involving natural convection in porous medium is those related to geothermal energy systems. The heat loss from the geothermal systems in some cases can be treated as if the heat comes from the heat generating sources. Studies have been made by several authors notably Hazem (2008) who analysed the effect of Hall current on transient hydromagnetic Coquette-Poiseuille flow of a viscoelastic fluid with heat transfer. Anwar et al (2010) studied magnetro hydrodynamic viscous plasma flow in rotating porous media with Hall currents and inclined magnetic field influence.

The resulting dimensionless ordinary differential equations were solved using the network simulation method. Both the primary and secondary flow velocities were found to increase with increased Darcy number values and increasing pressure gradient parameter but decreased with a rise in Hartmann number.

Abuga et al (2011) studied the effect of hall current and rotational parameter on dissipative fluid flow past a vertical semi-infinite plate. It was observed that an increase in Hall parameter for both cooling and heating of the plate by free convection currents led to an increase in the velocity profiles. Jordan (2007) analysed the effect of thermal radiation and viscous dissipation on MHD free convection flow over a semi- infinite vertical porous plate.

The network simulation method was used to solve the boundary layer equation based on the finite difference formulation. It was found that an increase in viscous dissipation leads to an increase of both velocity and temperature profiles.

Srinivasa et al (2011) considered thermo-diffusion effect on mixed convective heat and mass transfer flow of a viscous dissipative fluid through a porous medium in a non-uniform heated vertical channel. The governing equations for this investigation were solved numerically and it was found that the magnitude of velocity u increases with increase in Reynolds number R , an increase in Sc enhances v in the region except in the vicinity of the right boundary and the variation of u with buoyancy ratio N increases.

Das et al (2009) investigated mass transfer effects on MHD flow and heat transfer past a vertical porous plate through a porous medium under oscillatory suction and heat source.

The solutions for velocity field, temperature field and concentration distribution were obtained using perturbation technique and it was observed that the magnetic parameter and Schmidt number retard the velocity of the flow field while the Grashof number for heat and mass transfer, the porosity parameter and the heat source parameter have accelerating effect on the velocity of the flow field at all points. Further, the Prandtl number reduces the temperature and the Schmidt number diminishes the concentration of the flow fields at all points.

Sweet et al (2011) studied the analytical solution for the unsteady MHD flow of a viscous fluid between moving parallel plates. They discovered that an increase in the fluid density corresponded to a decrease in the velocity along the y-direction and that the initial velocity in the x-direction decreased with an increase in the fluid density.

Palani et al. (2009) studied MHD flow past a semi-infinite vertical plate with mass transfer and it was observed that the magnetic parameter M has a retarding effect on velocity. However, the effect of viscous dissipative incompressible heat that is generating fluid with mass and heat transfer has received little attention hence the present study is attempted.

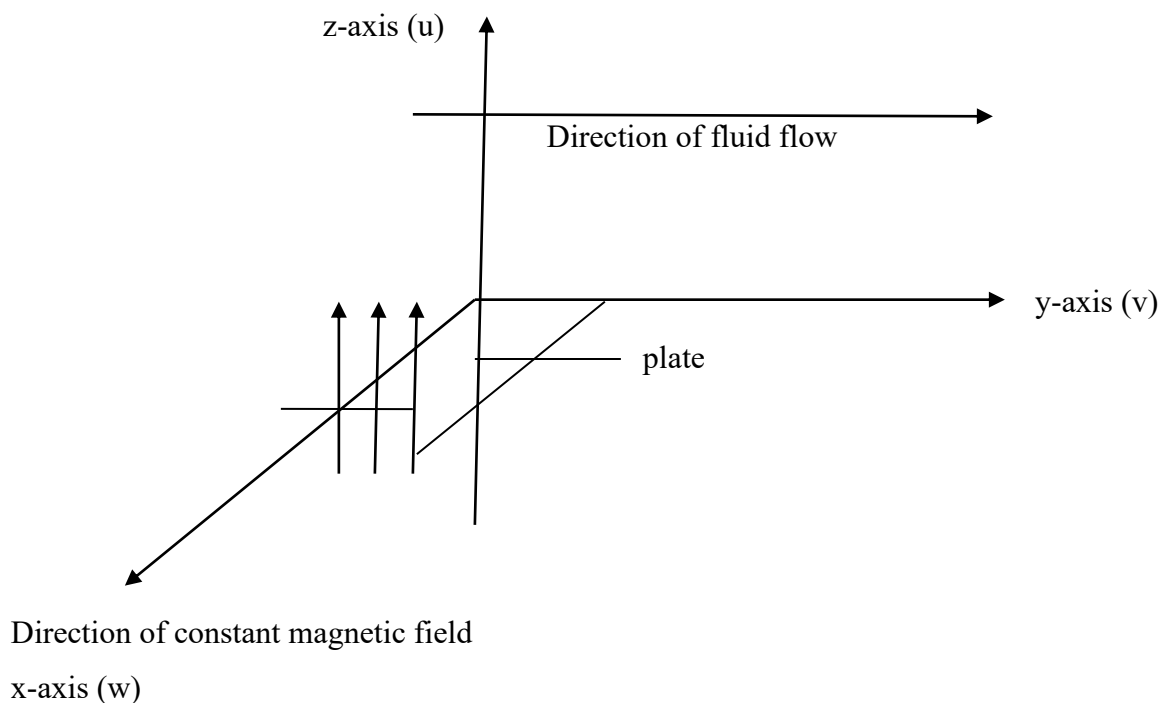


Fig. 1 Flow configuration

2. Specific equations governing fluid flow

In this section, the specific equations governing dissipative incompressible heat generating fluid with mass and heat transfer are considered.

In particular, an incompressible magnetohydrodynamic flow past a semi-infinite horizontal plate subject to a strong field is studied.

The y-axis is taken to be the direction of the fluid flow, z-axis the direction of the magnetic field. The z-axis is normal to the plate, and since the plate is semi-infinite in length, for a two dimensional incompressible fluid flow, the physical variables are functions of x, z and t. On application of the flow geometry to the general governing equations subject to certain conditions, the model equations governing the flow becomes:

$$\left[\frac{\partial u^+}{\partial t^+} + u^+ \frac{\partial u^+}{\partial x^+} - W_0^+ \frac{\partial u^+}{\partial z^+} \right] = \nu \left[\frac{\partial^2 u^+}{\partial x^{+2}} + \frac{\partial^2 u^+}{\partial z^{+2}} \right] + \beta g(T^+ - T_\infty^+) + \beta^* g(C^+ - C_\infty^+) - \frac{\sigma \mu_e^2 H_z^2 u^+}{\rho} \quad (1)$$

$$\left[\frac{\partial v^+}{\partial t^+} + u^+ \frac{\partial v^+}{\partial x^+} - W_0^+ \frac{\partial v^+}{\partial z^+} \right] = \nu \left[\frac{\partial^2 v^+}{\partial x^{+2}} + \frac{\partial^2 v^+}{\partial z^{+2}} \right] - \frac{\sigma \mu_e^2 H_z^2 v^+}{\rho} \quad (2)$$

$$\left[\frac{\partial T^+}{\partial t^+} + u^+ \frac{\partial T^+}{\partial x^+} - W_0^+ \frac{\partial T^+}{\partial z^+} \right] = \frac{1}{\rho C_p} \left\{ k \left[\frac{\partial^2 T^+}{\partial x^{+2}} + \frac{\partial^2 T^+}{\partial z^{+2}} \right] + Q^+ + \mu \left[\left(\frac{\partial u^+}{\partial z^+} \right)^2 + \left(\frac{\partial v^+}{\partial z^+} \right)^2 \right] \right\} \quad (3)$$

$$\left[\frac{\partial c^+}{\partial t^+} + u^+ \frac{\partial c^+}{\partial x^+} - W_0^+ \frac{\partial c^+}{\partial z^+} \right] = D \left[\frac{\partial^2 c^+}{\partial x^{+2}} + \frac{\partial^2 c^+}{\partial z^{+2}} \right] \quad (4)$$

Letting all the variables with superscript plus (+) to represent dimensional variables, then the non-dimensionalization is based on the following general scaling variables.

$$t = \frac{t^+ U^2}{\nu}, \quad x = \frac{x^+ U}{\nu}, \quad z = \frac{z^+ U}{\nu}, \quad u = \frac{u^+}{U}, \quad v = \frac{v^+}{U}, \quad w = \frac{W_0^+}{U}, \quad \theta = \frac{T^+ - T_\infty^+}{T_w^+ - T_\infty^+}, \quad C = \frac{C^+ - C_\infty^+}{C_w^+ - C_\infty^+},$$

$$\sigma = \frac{Q^+ \nu^2}{K U^2}$$

U is the characteristic velocity

$T_w^+ - T_\infty^+$ is the temperature difference between the surface and free stream temperature

$C_w^+ - C_\infty^+$ is the concentration difference between the concentration at the surface and the free stream concentration.

Equations (1), (2), (3) and (4) can be written using dimensional variables as

$$\frac{\partial u}{\partial t} + u \frac{\partial u}{\partial x} - W_0 \frac{\partial u}{\partial z} = \left[\frac{\partial^2 u}{\partial x^2} + \frac{\partial^2 u}{\partial z^2} \right] + Gr\theta + GcC - M^2u \quad (5)$$

$$\frac{\partial v}{\partial t} + u \frac{\partial v}{\partial x} - W_0 \frac{\partial v}{\partial z} = \left[\frac{\partial^2 v}{\partial x^2} + \frac{\partial^2 v}{\partial z^2} \right] - M^2v \quad (6)$$

$$\frac{\partial \theta}{\partial t} + U \frac{\partial \theta}{\partial x} - w_0 \frac{\partial \theta}{\partial z} = \frac{1}{Pr} \left(\frac{\partial^2 \theta}{\partial x^2} + \frac{\partial^2 \theta}{\partial z^2} \right) + \frac{\sigma \theta}{Pr} + Ec \left[\left(\frac{\partial u}{\partial z} \right)^2 + \left(\frac{\partial v}{\partial z} \right)^2 \right] \quad (7)$$

$$\frac{\partial C}{\partial t} + u \frac{\partial C}{\partial x} - W_0 \frac{\partial C}{\partial z} = \frac{1}{Sc} \left(\frac{\partial^2 C}{\partial x^2} + \frac{\partial^2 C}{\partial z^2} \right) \quad (8)$$

3. Method of Solution

Equations governing dissipative incompressible fluid flow considered in this study are non-linear thus their exact solution is not possible. In order to solve these equations, a fast and stable method for the solution of finite difference approximation has been employed in order to satisfy basic requirements such as consistency, stability and convergence.

A method is consistent if as more grid points are taken or step size decreased, the truncation error tends to zero. A method is stable if the effect of any single fixed round off error is bounded and finally a method is convergent if the numerical solution converges to the exact solution. The numerical error arises because in most computations we cannot exactly compute the difference solution as we encounter round off errors.

If the effects of the round off error remains bounded as the mesh point tend to infinity with fixed step size, then the difference method is said to be stable. In order to approximate equations (5), (6), (7) and (8) by a set of finite difference equations, we first define a suitable mesh.

3.1 Mesh point

In order to give a relationship between the partial derivatives in the differential equation and the function values at the adjacent nodal points, a uniform mesh was used. Let the x-z plane be divided into a network of uniform rectangular cells of width Δz and height Δx as shown below. k and i refer to the z and x axis respectively

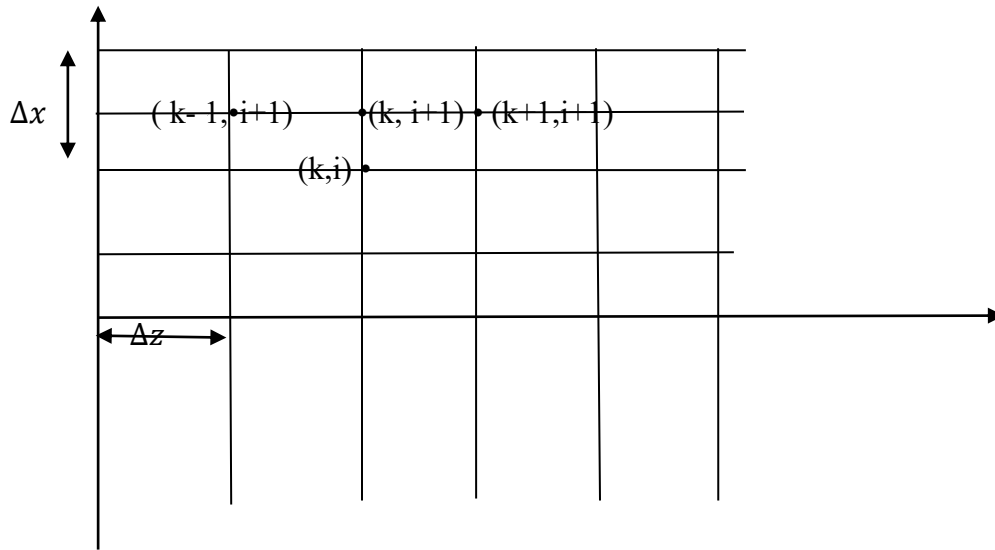


Fig. 2 mesh point

Let Δz represent increment in z and Δx represent increment in x then $z = k\Delta z$ and $x = i\Delta x$. The finite difference approximations of the partial derivatives appearing in equations (5), (6), (7) and (8) are obtained by Taylor's series expansion of the dependent variable about a grid point (k, i) as,

$$\phi(k-1, i) = \phi(k, i) - \phi'(k, i)\Delta z + \frac{1}{2}\phi''(k, i)(\Delta z)^2 - \frac{1}{6}\phi'''(k, i)(\Delta z)^3 + \dots \quad (9)$$

$$\phi(k+1, i) = \phi(k, i) + \phi'(k, i)\Delta z + \frac{1}{2}\phi''(k, i)(\Delta z)^2 + \frac{1}{6}\phi'''(k, i)(\Delta z)^3 + \dots \quad (10)$$

Subtracting equation (9) from (10) to eliminate ϕ'' we get

$$\phi' = \frac{\phi(k+1, i) - \phi(k-1, i)}{2\Delta z} + Hot \quad (11)$$

Adding equation (9) to (10) to eliminate ϕ' we get

$$\phi'' = \frac{\phi(k+1, i) - 2\phi(k, i) + \phi(k-1, i)}{(\Delta z)^2} + Hot \quad (12)$$

Central difference formulae for the first and second derivatives with respect to x are

$$\phi' = \frac{\phi(k, i+1) - \phi(k, i-1)}{2\Delta x} + Hot \quad (13)$$

$$\phi'' = \frac{\phi(k, i+1) - 2\phi(k, i) + \phi(k, i-1)}{(\Delta x)^2} + Hot \quad (14)$$

In this study, the subscripts used indicate spatial points. Let the mesh point variable at time t be denoted by $\phi_{(k,i)}$. The forward difference for the first order derivatives with respect to time t is given by

$$\phi'_{(k,i)} = \frac{\phi_{(k,i+1)} - \phi_{(k,i)}}{\Delta t} + Hot \tag{15}$$

Using the forward finite difference for the first order time derivative and central finite difference for the first and second order spatial derivative, the final set of the governing equations from equations (5), (6), (7) and (8) in finite difference form are,

$$u_{(k,i+1)} = \Delta t \left\{ -u_{(k,i)} \left[\frac{u_{(k,i+1)} - u_{(k,i-1)}}{2\Delta x} \right] + W_0 \left[\frac{u_{(k+1,i)} - u_{(k-1,i)}}{2\Delta z} \right] + \left[\frac{u_{(k+1,i)} - 2u_{(k,i)} + u_{(k-1,i)}}{(\Delta z)^2} \right] + \left[\frac{u_{(k,i+1)} - 2u_{(k,i)} + u_{(k,i-1)}}{(\Delta x)^2} \right] + Gr\theta_{(k,i)} + GcC_{(k,i)} - M^2 u_{(k,i)} \right\} + u_{(k,i)} \tag{16}$$

$$v_{(k,i+1)} = \Delta t \left\{ -u_{(k,i)} \left[\frac{v_{(k,i+1)} - v_{(k,i-1)}}{2\Delta x} \right] + W_0 \left[\frac{v_{(k+1,i)} - v_{(k-1,i)}}{2\Delta z} \right] + \left[\frac{v_{(k+1,i)} - 2v_{(k,i)} + v_{(k-1,i)}}{(\Delta z)^2} \right] + \left[\frac{v_{(k,i+1)} - 2v_{(k,i)} + v_{(k,i-1)}}{(\Delta x)^2} \right] - M^2 v_{(k,i)} \right\} + v_{(k,i)} \tag{17}$$

$$\theta_{(k,i+1)} = \Delta t \left\{ -u_{(k,i)} \left[\frac{\theta_{(k,i+1)} - \theta_{(k,i-1)}}{2\Delta x} \right] + W_0 \left[\frac{\theta_{(k+1,i)} - \theta_{(k-1,i)}}{2\Delta z} \right] + \frac{1}{Pr} \left[\frac{\theta_{(k,i+1)} - 2\theta_{(k,i)} + \theta_{(k,i-1)}}{(\Delta x)^2} \right] + \frac{1}{Pr} \left[\frac{\theta_{(k+1,i)} - 2\theta_{(k,i)} + \theta_{(k-1,i)}}{(\Delta z)^2} \right] - \frac{\delta}{Pr} \theta_{(k,i)} + Ec \left[\frac{\theta_{(k+1,i)} - \theta_{(k-1,i)}}{2\Delta z} \right]^2 + Ec \left[\frac{\theta_{(k,i+1)} - \theta_{(k,i-1)}}{2\Delta x} \right]^2 \right\} + \theta_{(k,i)} \tag{18}$$

$$C_{(k,i+1)} = \Delta t \left\{ -u_{(k,i)} \left[\frac{C_{(k,i+1)} - C_{(k,i-1)}}{2\Delta x} \right] + W_0 \left[\frac{C_{(k+1,i)} - C_{(k-1,i)}}{2\Delta z} \right] + \frac{1}{Sc} \left[\frac{C_{(k,i+1)} - 2C_{(k,i)} + C_{(k,i-1)}}{(\Delta x)^2} \right] + \frac{1}{Sc} \left[\frac{C_{(k+1,i)} - 2C_{(k,i)} + C_{(k-1,i)}}{(\Delta z)^2} \right] \right\} + C_{(k,i)} \tag{19}$$

The initial conditions take the form

$$\text{At } z = 0, u_{(0,i)} = 1, v_{(0,i)} = 1, \theta_{(0,i)} = 1, C_{(0,i)} = 1$$

$$\text{At } z > 0, u_{(k,i)} = 1, v_{(k,i)} = 1, \theta_{(k,i)} = 1, C_{(k,i)} = 1$$

For $k > 0$ and all i .

The boundary conditions take the form;

Ec=100	Ec=1
0	0
-2.52E-10	-2.52E-10
1.84E-13	1.84E-13
-1.34E-16	-1.34E-16
9.74E-20	9.74E-20

At $z = 0$, $u_{(0,i)} = 0, v_{(0,i)} = 0, \theta_{(0,i)} = 0, C_{(0,i)} = 0$

At $x = 0$, $u_{(k,0)} = 1, v_{(k,0)} = 1, \theta_{(k,0)} = 1, C_{(k,0)} = 1$

Computations were done for $\theta_{(k,i+1)}$ and $C_{(k,i+1)}$ from equations (18) and (19) respectively. During the computations, the Prandtl number was taken as 0.71 which corresponds to air, magnetic parameter $M^2 = 5$ which signifies a strong magnetic field.

The computations were performed using small values of $\Delta x = 0.012$ and $\Delta z = 0.25$ to ensure stability, consistence and convergence of the finite difference method.

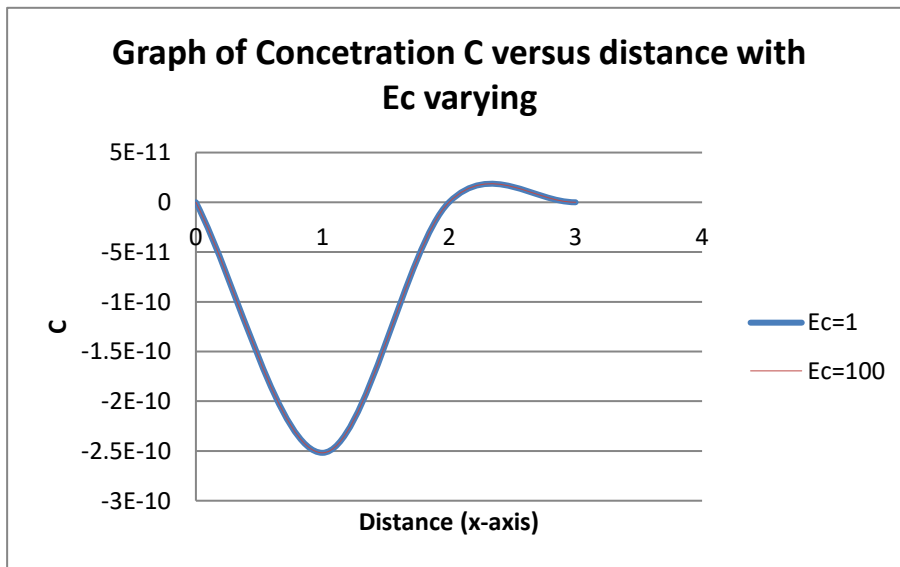
4. Results and Discussion

In the discussion of the results, a programming language called Java is used to find values of temperature and concentration for the finite difference equations (18) and (19) for values of Schmidt parameters 50 to 5000 and Eckert parameter 1 to 100. The temperature and concentration profiles are presented graphically in figures 3 to 6 and numerical data in tables 1 to 4.

Table 1: Concentration Profile (Ec varying)

-7.09E-23	-7.09E-23
5.16E-26	5.16E-26
-3.75E-29	-3.75E-29
2.71E-32	2.71E-32
-1.95E-35	-1.95E-35
1.39E-38	1.39E-38
-9.88E-42	-9.88E-42
6.95E-45	6.95E-45
-4.84E-48	-4.84E-48
3.35E-51	3.35E-51
-2.29E-54	-2.29E-54
1.56E-57	1.56E-57

Figure 3: Graph of Concentration profile (Ec varying)



From table 1 and graph in figure 3 above, it is observed that as the Ec number increases from 1 to 100, the Concentration profiles decreases at a small distance of the fluid from the plate and as the distance increases From the plate, the concentration profile increases.

Table 2: Concentration profile with Sc varying

Sc=50	Sc=5000
0	0
-2.52E-10	-2.52E-10
-1.34E-14	-1.34E-10
9.75E-17	9.75E-11
-7.10E-19	-7.10E-11
5.17E-21	5.17E-11
-3.76E-23	-3.76E-11
2.72E-25	2.72E-11
1.40E-29	1.40E-11
-9.93E-32	-9.93E-12
6.98E-34	6.98E-12
-4.87E-36	-4.87E-12
3.37E-38	3.37E-12
-2.31E-40	-2.31E-12
1.57E-42	1.57E-12
-1.06E-44	-1.06E-12
7.11E-47	7.11E-13
-4.73E-49	-4.73E-13
3.12E-51	3.12E-13
-2.05E-53	-2.05E-13
1.34E-55	1.34E-13
-8.67E-58	-8.67E-14
5.60E-60	5.60E-14
-3.59E-62	-3.59E-14

From table 2 and the graph in figure 4 above, it is observed that an increase in mass diffusion parameter Sc which is the ratio of kinematic viscosity to mass diffusivity from 50 to 5000 leads to an increase in concentration profile a short distance away from the plate and as the distance

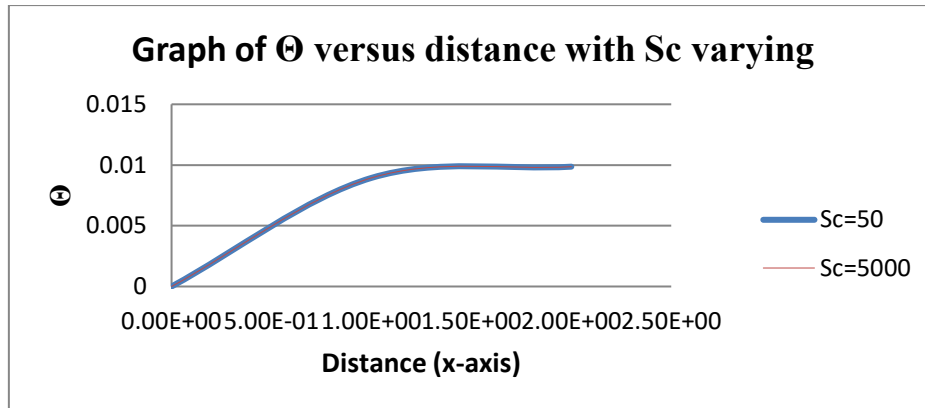
increases the concentration profile decreases exponentially. This is because Sc is directly proportional to dynamic viscosity which is a measure of shear stress and inversely proportional to density which is assumed to be a constant and mass diffusivity, due to the fact that mass diffusion parameter Sc is inversely proportional to mass diffusivity then, an increase in Sc results into a decrease in concentration profile as distance of the fluid flow away from the plate increases.

Table 3: Temperature profile (Sc varying).

Temperature, Θ		
	$Sc=50$	$Sc=5000$
0.00E+00	0	0
1.00E+00	8.94E-03	8.94E-03
2.00E+00	9.86E-03	9.86E-03
3.00E+00	1.09E-02	1.09E-02
4.00E+00	1.19E-02	1.19E-02

$Sc=50$	$Sc=5000$
0	0
-8.45E-03	-8.45E-03
8.94E-03	8.94E-03
-9.39E-03	-9.39E-03
9.86E-03	9.86E-03
-1.04E-02	-1.04E-02
1.09E-02	1.09E-02
-0.01139	-0.01139
1.19E-02	1.19E-02

Figure 5: Temperature profile (θ –graph) with Sc varying



From table 3 and the graph in figure 5 above, it is observed that as Sc number increases from 50 to 5000 the temperature profile increases exponentially. Similarly as the distance of the fluid flow from the plate increases, the temperature profile also increases. Sc number gives the ratio of kinematic viscosity and mass diffusivity and therefore when mass diffusivity is decreased, Sc number increases since the two are inversely proportional to each other. Hence decreasing mass diffusivity D increases the mass diffusion parameter Sc consequently leading to an increase in temperature profiles.

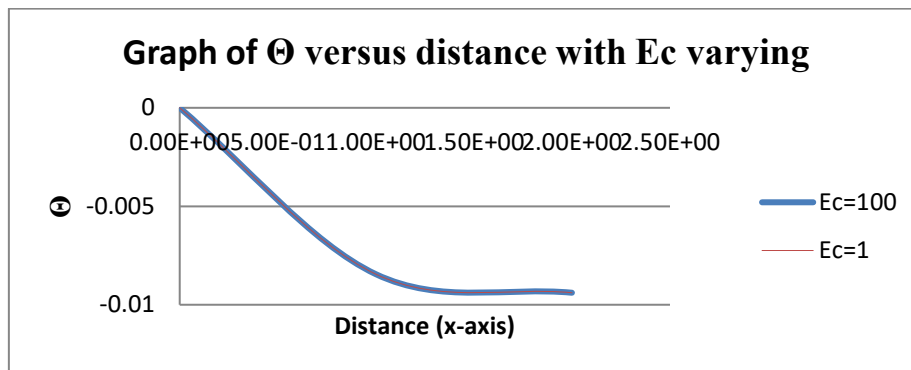
Table 4: Temperature profile (Ec varying)

Temperature, Θ		
	Ec=100	Ec=1
0.00E+00	0	0
1.00E+00	-8.45E-03	-8.45E-03
2.00E+00	-9.39E-03	-9.39E-03
3.00E+00	-1.04E-02	-1.04E-02
4.00E+00	-1.139E-02	-1.139E-02
5.00E+00	-1.23E-02	-1.23E-02

Ec=100	Ec=1
0	0
-8.45E-03	-8.45E-03

8.94E-03	8.94E-03
-9.39E-03	-9.39E-03
9.86E-03	9.86E-03
-1.04E-02	-1.04E-02
1.09E-02	1.09E-02
-0.01139024	-0.01139024
1.19E-02	1.19E-02

Figure 6: Temperature profile (θ –graph) with Ec varying



From table 4 above and the graph in figure 6 above, it is observed that as Eckert number Ec decreases from 100 to 1 the temperature profile decreases a distance from the plate and as the distance of the fluid flow increases from the plate, temperature profile decreases. Since Ec is inversely proportional to thermal energy then increasing thermal energy leads to a decrease in Ec number and consequently decreasing the temperature profile as depicted in the exponential graph.

5. Conclusion

An analysis of the effects of Schmidt and Eckert parameters on temperature and concentration profiles on dissipative incompressible heat generating fluid with mass and heat transfer has been carried out. In the presence of mass and heat transfer, increase in mass diffusion parameter Sc leads to a increase in temperature and concentration profiles but away from the plate, along the x -axis, the concentration profile decreases. Similarly, an increase in viscous dissipative heat, Ec leads to a decrease in concentration profile while the temperature profile increases but a distance

away from the plate along the x-direction, the concentration profile increases while the temperature profile remains constant.

References

1. Abuga J.G, Kinyanjui M. And Sigey J.K. An investigation of the effect of hall current and rotational parameter on dissipative fluid flow past a vertical semi-infinite plate. *Journal of Engineering and Technology Research* vol.3 (11), pp. 314-320, October 2011.
2. Anwar Beg O, Lik S, Zueco J and Bhargava R. Numerical study of magnetohydrodynamic viscous plasma flow in rotating porous media with Hall currents and inclined magnetic field influence. *Common Nonlinear Sci Numer Simulat* 15 (2010) 345-359)
3. Das S.S, Satapathy A. Das J.K, and Panda J.P. Mass transfer effects on MHD flow and heat transfer past a vertical porous plate through a porous medium under oscillatory suction and heat source. *International journal of heat and mass transfer* 52 (2009) 5962-5969.
4. Hazem, A.A. (2008). Effect of hall current on transient hydromagnetic Couette-Poiseuille flow of a viscoelastic fluid with heat transfer. *Appl. Math. Model*, 32(4): 375-388.
5. Jordan J.Z. Network simulation method applied to radiation and viscous dissipation effects on MHD unsteady free convection over vertical porous plate. *Applied mathematical modelling* Vol. 31 P.2019-2033 (2007).
6. Palani G,Srikanth U (2009). MHD flow past a semi-infinite vertical plate with mass transfer Non-linear Analysis; *Model. Control*, 14(3): 345-356
7. Srinivasa Rao P, Reddaiah, P and Sreenivas, G. (2011). Thermo-diffusion effect on mixed convective heat and mass transfer flow of a viscous dissipative fluid through a porous medium in a non-uniformly heated vertical channel *International journal of applied mathematics and Mechanics* (2011) 75-95.
8. Sweet E, Vajravelu K, Robert A and Van Gorder P (2011). Analytical solution for the unsteady MHD flow of a viscous fluid between moving parallel plates. *Commun. Sci. Numer. Simul.* 16: 266-273.